



This is a repository copy of *Development of a creep-free stress-strain law for fire analysis of steel structures*.

White Rose Research Online URL for this paper:  
<http://eprints.whiterose.ac.uk/105287/>

Version: Accepted Version

---

**Article:**

Torić, N., Sun, R.R. and Burgess, I.W. [orcid.org/0000-0001-9348-2915](https://orcid.org/0000-0001-9348-2915) (2016)  
Development of a creep-free stress-strain law for fire analysis of steel structures. *Fire and Materials*, 40 (7). pp. 896-912. ISSN 0308-0501

<https://doi.org/10.1002/fam.2347>

---

This is the peer reviewed version of the following article: Torić, N., Sun, R. R., and Burgess, I. W. (2015) Development of a creep-free stress-strain law for fire analysis of steel structures. *Fire Mater.*, which has been published in final form at doi: 10.1002/fam.2347. This article may be used for non-commercial purposes in accordance with Wiley Terms and Conditions for Self-Archiving.

**Reuse**

Unless indicated otherwise, fulltext items are protected by copyright with all rights reserved. The copyright exception in section 29 of the Copyright, Designs and Patents Act 1988 allows the making of a single copy solely for the purpose of non-commercial research or private study within the limits of fair dealing. The publisher or other rights-holder may allow further reproduction and re-use of this version - refer to the White Rose Research Online record for this item. Where records identify the publisher as the copyright holder, users can verify any specific terms of use on the publisher's website.

**Takedown**

If you consider content in White Rose Research Online to be in breach of UK law, please notify us by emailing [eprints@whiterose.ac.uk](mailto:eprints@whiterose.ac.uk) including the URL of the record and the reason for the withdrawal request.



[eprints@whiterose.ac.uk](mailto:eprints@whiterose.ac.uk)  
<https://eprints.whiterose.ac.uk/>

# DEVELOPMENT OF A CREEP-FREE STRESS-STRAIN LAW FOR FIRE ANALYSIS OF STEEL STRUCTURES

Neno Torić<sup>1\*</sup>, Rui Rui Sun<sup>2</sup> and Ian W. Burgess<sup>3</sup>

## Abstract:

This paper presents a practical procedure for obtaining creep-free stress-strain laws for steel exposed to fire, on the basis of codified stress-strain laws which consider creep implicitly. The applicability of the proposed procedure has been tested on two commonly used stress-strain laws for steel at elevated temperature; the Eurocode 3 law and a Ramberg-Osgood model, both of which have implicit consideration of creep. The simulation of two published steel coupon experiments on steel of grades S275 and S355 shows that both the Eurocode and Ramberg-Osgood stress-strain laws produce inaccurate predictions of creep in fire at elevated temperatures. The proposed procedure was thereby used to extract the implicit creep according to the heating rates of the transient coupon tests, and to derive the creep-free stress-strain laws. It has been shown that, by combining the creep-free stress strain law obtained by the proposed methodology with an explicit creep model, a more realistic prediction of steel behaviour in the selected coupon test studies can be achieved.

## Keywords:

Steel, creep, fire, beam, finite element, coupon, creep-free

---

<sup>1</sup> University of Split, Faculty of Civil Engineering, Architecture and Geodesy, Matice Hrvatske 15, 21000 Split, Croatia, Tel: +385-21-303-366, Fax: +385-21-303-331

\* E-mail: neno.toric@gradst.hr (corresponding author)

<sup>2</sup> MMI Engineering, AVC Business Centre, Wellington Circle, Aberdeen, AB12 3JG, UK.

<sup>3</sup> University of Sheffield, Department of Civil and Structural Engineering, Sir Frederick Mappin Building, Mappin Street, Sheffield, S1 3JD, UK.

# 1. INTRODUCTION

Fundamental stress-strain laws for steel at elevated temperatures can be determined using two different testing methods; stationary and transient testing. A law derived from transient tests normally contains some creep strain within its total strain, which is dependent on their heating rates. This type of material law is generally considered as one which includes creep strain in an implicit manner. At present, stress-strain relationships which originate from steady-state tests are not codified, nor are they generally used in performance-based fire engineering in Europe. However it is important to note that Poh [1] has proposed a stress-strain law for use in high-temperature engineering analysis which is considered to be creep-free since it is based on test results of steady-state-heated coupons conducted with fast strain rates. A stress-strain model similar to Poh's, with a sharp transition between the elastic and plastic phases, has been proposed by ASCE [2] for engineering analysis. This type of stress-strain model might be considered as a creep-free model due to lack of curved part between these two phases since implicit creep tends to increase the curvature of the stress-strain characteristic. The objective of this study is focused on the analysis of contemporary stress-strain curves which are predominantly used in Europe.

An implicit material law is considered as a conservative representation according to current structural design codes in Europe [3, 4] in which no explicit creep model is required for a structural fire analysis. Recent research studies [5, 6, 7, 8, 9, 10] have shown that additional consideration of creep strains, either explicit or implicit, is necessary in structural fire analysis in cases where steel members are kept at temperatures above about one third of the melting temperature for a prolonged time period. However, the implicit constitutive stress-strain law from Eurocode 3 cannot account for the realistic development of creep strains [5, 7, 10] in cases of prolonged heat exposure above 400°C, which is generally considered as the temperature at which creep strain starts to evolve (in some structures such as chimneys and heat ducts creep starts to evolve at about 100°C). This suggests that implicit stress-strain laws can not necessarily lead to conservative predictions of the creep

strain in steel for all possible heating rates, particularly for members exposed to slow heating rates below 20°C/min.

In order to predict the creep in steel accurately, a stress-strain law with implicit consideration of creep cannot be combined with any explicit creep model, because this will usually overstate the creep strains. Therefore, a suitable creep-free stress-strain material law is a vital need for an analysis of steel structures in fire which needs to predict creep strains explicitly. The objective of this research is to provide a practical procedure to derive a creep-free stress-strain law from the existing stress-strain laws that are commonly used in the performance-based structural fire engineering. The procedure presented here is capable of estimating the implicit creep strain from a transient-test-based stress-strain law, and can be applied to any kind of stress-strain law of steel with implicit consideration of creep.

The procedure has been implemented in the Vulcan research code using three different explicit creep models. The Ramberg-Osgood and Eurocode 3 stress-strain laws have been selected for verification of the proposed methodology. It has then been validated against the results from two previously published experimental coupon studies which are focused on two common contemporary Eurocode 3 steel grades; S275 and S355.

## **2. DEVELOPMENT OF A CREEP-FREE STRESS-STRAIN LAW**

### **2.1 Explicit creep analysis**

Within the scope of the presented research, three widely-used creep models, based on either time-hardening or strain-hardening rules, were utilized to predict the creep strains of steel at elevated temperature. A time-hardening creep model, in which creep strain rate is regarded as a function of stress and time, is applicable when the stress level during fire exposure remains approximately constant. A strain-hardening creep model is applicable when the stress changes during fire exposure, which makes the creep strain rate a function

of previously accumulated creep strain and stress. The details of the three creep models are given in this section.

The first creep model (Cr\_1) is based on a strain-hardening rule, and was developed by Harmathy [11]. The creep strain rate can be expressed as:

$$\frac{\Delta \varepsilon_{cr}}{\Delta t} = Z \cdot \exp\left(-\frac{\Delta H}{RT_R}\right) \cdot \coth^2\left(\frac{\varepsilon_{cr,c}}{\varepsilon_{cr,0}}\right) \quad (1)$$

where  $\frac{\Delta \varepsilon_{cr}}{\Delta t}$  is the creep strain rate,  $T_R$  is the temperature (°K),  $R$  is the universal gas constant (J/mol °K),  $\Delta H$  is the creep activation energy (J/mol),  $Z$  is the Zener-Hollomon parameter ( $h^{-1}$ ),  $\varepsilon_{cr,0}$  is a dimensionless creep parameter,  $\varepsilon_{cr,c}$  is previously accumulated creep strain, and  $\Delta t$  (h) is the time increment. The creep strain increase in the time increment  $\Delta t$  is obtained by integration of the expression (1) with respect to time.

The second creep model (Cr\_2) was also developed by Harmathy [12], but is based on a time-hardening rule. The creep strain can be expressed as:

$$\varepsilon_{cr} = \frac{\varepsilon_{cr,0}}{0.693} \cdot \cosh^{-1}\left(2^{\frac{\theta}{\theta_0}}\right) \quad (\theta < \theta_0) \quad (2)$$

$$\varepsilon_{cr} = \varepsilon_{cr,0} + Z\theta \quad (\theta \geq \theta_0) \quad (3)$$

$$\theta_0 = \varepsilon_{cr,0} / Z \quad (4)$$

in which  $\theta$  represents temperature-compensated time. This takes into account the variation with time of temperature, and can be expressed in integral form as:

$$\theta = \int_0^t \exp^{\frac{-\Delta H}{RT_R}} dt \quad (5)$$

Integration of Equation (5) is conducted using the following expression:

$$\theta_{t_i} = \theta_{t_{i-1}} + \theta_{\Delta t} = \theta_{t_{i-1}} + \exp^{\frac{-\Delta H}{RT_R}} \Delta t \quad (6)$$

Temperature-compensated time  $\theta_{t_i}$  is used in Equation (2) in order to obtain the total creep strain in time  $t_i = t_{i-1} + \Delta t$ .

The third creep model (Cr\_3) was developed by Plem [13], and is based on a strain-hardening rule:

$$\varepsilon_{cr} = \varepsilon_{cr,0} (2\sqrt{Z\theta / \varepsilon_{cr,0}}) \quad (0 \leq \theta < \theta_0) \quad (7)$$

$$\varepsilon_{cr} = \varepsilon_{cr,0} + Z\theta \quad (\theta \geq \theta_0) \quad (8)$$

Temperature-compensated time  $\theta$  in Plem's model is calculated using:

$$\theta = \theta^0 + \exp^{\frac{\Delta H}{RT_r}} \Delta t \quad (9)$$

in which  $\theta^0$  represents a shifted temperature-compensated time, which is a function of the previously accumulated creep strain. This is determined using the following expressions:

$$\theta^0 = \frac{\varepsilon_c^{0^2}}{4\varepsilon_{cr,0}^0 Z} \quad (\varepsilon_c^0 < 2\varepsilon_{cr,0}) \quad (10)$$

$$\theta^0 = \frac{\varepsilon_c^0 - \varepsilon_{cr,0}}{Z} \quad (\varepsilon_c^0 \geq 2\varepsilon_{cr,0}) \quad (11)$$

where  $\varepsilon_c^0$  represents the creep strain from the previous time increment.

In order to utilize the chosen creep models, a range of material parameters for the appropriate steel grade has to be provided. Material parameters  $Z$ ,  $\Delta H/R$  and  $\varepsilon_{cr,0}$  are borrowed from a research study conducted by Harmathy and Stanzak [14]. For American A36 steel, which corresponds to the Eurocode steel grade S275, material parameters are given as follows:

$$\varepsilon_{cr,0} = 1.03 \cdot 10^{-6} \sigma^{1.75} \quad (12)$$

$$Z = 3.75 \cdot 10^8 \sigma^{4.7} \quad (\sigma \leq 103 \text{ MPa}) \quad (13)$$

$$Z = 1.23 \times 10^{16} \exp^{0.0435\sigma} \quad (103 < \sigma \leq 310 \text{ MPa}) \quad (14)$$

$$\frac{\Delta H}{R} = 38900 \text{ K} \quad (15)$$

## 2.2 Implicit stress-strain material law

In order to give a clear view of the different concepts involved in this study, several definitions of the material stress-strain curves are given as follows:

1. Implicit (“skeleton”) stress-strain laws: material laws which implicitly include consideration of creep. Examples are the Eurocode 3 and Ramberg-Osgood stress-strain curves;
2. Creep-free stress-strain laws: material laws derived from the codified material stress-strain curves by subtracting the creep strain components.

In this study, two implicit stress-strain laws (Eurocode 3 [3] and smoothed Ramberg-Osgood [15]) were used as experimental bases for testing the creep-free methodology. A smoothed Ramberg-Osgood stress-strain law is based on a fit of experimental data to a Ramberg-Osgood expression using temperature-dependent parametric functions [15, 16]. This can be considered as a material law which includes creep implicitly, since it has been used in a previous study by Mäkeläinen et al. [17] to produce stress-strain curves based on transient tests conducted at a heating rate of 10°C/min.

A set of Eurocode 3 temperature-dependent stress-strain curves was constructed on the basis of a series of transient tests conducted by Kirby and Preston [18] at a heating rate of 10°C/min. Since both of the chosen stress-strain laws were based on transient test results, they fit well with the objective of testing the methodology developed in this study.

## 2.3 Creep-free stress-strain material law

The procedure to derive the creep-free material stress-strain law from an existing codified stress-strain relationship consists of the following tasks:

1. Simulation of a series of transient coupon tests conducted with a certain heating rate (10°C/min in this particular study) at different stress levels in order to obtain a set of temperature-creep strain curves;
2. Creation of a set of stress-creep strain curves at different temperature levels by reinterpreting predetermined temperature-creep strain curves at constant stress;

3. Subtraction of creep strain values from the skeleton stress-strain curves, depending on the level of temperature and stress at any given time.

A schematic view of the creep-free methodology is given in Figure 1.

This proposed methodology can potentially be applied to material laws for any heating rate. However, this study is only focused on a representative heating rate of 10°C/min, since both the Eurocode 3 and Ramberg-Osgood material laws are based on tests conducted at this heating rate. Figure 2 presents examples of temperature-creep strain curves obtained by the proposed procedure on the basis of the Ramberg-Osgood skeleton curves for S275 steel. As shown in Figure 2, these temperature-creep strain curves are obtained using the three creep models implemented here with a heating rate of 10°C/min. It should be noted that different sets of temperature-creep strain curves can be created, depending on the nature of the skeleton law, the steel grade and the particular creep model used in the analysis.

Figure 3 presents a stress-creep strain curves at various temperature levels derived from the temperature-creep strain curves in Figure 2. It can be seen from Figure 3 that different combinations of skeleton laws and creep models lead to different sets of stress-creep strain curves, which will then generate different creep-free stress strain curves, even if based on the same skeleton curves.

## 2.4 Code implementation

Implementation of the creep models in the Vulcan research code has been conducted in an explicit manner, by including an additional term in the total strain formulation, which can be written in the following form [19]:

$$\varepsilon_{\text{tot}} = \varepsilon_{\text{th}}(\mathbf{T}) + \varepsilon_{\sigma}(\sigma, \mathbf{T}) + \varepsilon_{\text{cr}}(\sigma, \mathbf{T}, t) \quad (16)$$

in which:  $\varepsilon_{\text{tot}}$  is the total strain,  $\varepsilon_{\text{th}}(\mathbf{T})$  is the temperature-dependent thermal strain,  $\varepsilon_{\sigma}(\sigma, \mathbf{T})$  is the stress related strain (dependent upon applied stress  $\sigma$  and the temperature  $\mathbf{T}$ ) and  $\varepsilon_{\text{cr}}(\sigma, \mathbf{T}, t)$  is the creep strain (stress-, temperature- and time-dependent strain). The stress-related (mechanical) strains are determined by the material laws in fire. As stated previously, commonly-used skeleton stress-strain laws already contain implicit creep. In



order to achieve an accurate prediction of the total strain from Equation (16), the implicit consideration of creep in the skeleton stress-strain laws should be removed.

The creep-free methodology has been implemented in the Vulcan research code so that the total strain is expressed as:

$$\varepsilon_{\text{tot}} = \varepsilon_{\text{th}}(\mathbf{T}) + \varepsilon_{\sigma}(\sigma, \mathbf{T}) + \varepsilon_{\text{cr}}(\sigma, \mathbf{T}, t) - \varepsilon_{\text{impl,cr}}(\sigma, \mathbf{T}) \quad (17)$$

where:  $\varepsilon_{\text{impl,cr}}(\sigma, \mathbf{T})$  represents the projected implicit creep strain value which is calculated from the selected stress-creep strain curve as illustrated in Figure 3. The process reduces the stress-related strain value from that in the skeleton material law by the value of the predicted implicit creep at any stress and temperature level. The time-dependency of the fourth term in Equation (17) is not strictly necessary, since the objective of the creep-free methodology is to subtract the implicit creep which occurs at the prescribed heating rate of 10°C/min. Therefore, the time variable in the implicit creep function has already been taken into account in the first step of the creep-free procedure.

Subtracting the creep strain values from the skeleton curves avoids double-counting of the creep contribution to the total strain. As a result, a reduced stress-related strain is calculated at any time step in accordance with Equation (17).

## 2.5 Experimental studies

In order to verify the proposed creep-free methodology, two previously published experimental studies have been selected to model and compare. The former was conducted by Kirby and Preston [18], within which a comprehensive set of transient tests was conducted on steel coupons, at various heating rates between 2.5°C/min and 20°C/min. The steels tested were the UK grades 43A and 50B, which correspond to the Eurocode 3 grades S275 and S355 respectively. The latter was a less complete set of transient coupon tests conducted by Boko et al. [20]. These tests were conducted on S355 carbon steel at stress levels varying from 50-400 MPa and a single heating rate of 10°C/min.

One of the main reasons for selecting these two particular test programmes is that they both include the heating rate (10°C/min) used in the tests on which the Eurocode 3 and

Ramberg-Osgood stress-strain laws were based. This similarity reduces the discrepancies which might come from different heating rates.

## 2.6 Finite element modelling

The experimental tests mentioned above were modelled using Vulcan. Three-noded line elements from the Vulcan library [21, 22] were employed. Figure 4 shows the dimensions of the coupons used in Boko's study, and the finite element segmentation used for modelling their cross-sections.

Coupons with gauge lengths 40mm from the Kirby and Preston study and 98mm from Boko's study were modelled with two line elements and a cross-section divided into 8x8 segments. An iterative incremental calculation was carried out to obtain the coupon deformation  $\Delta l_t$ . Engineering strain was determined from

$$\varepsilon_{\text{gauge,t}} = \frac{\Delta l_t}{l} \quad (18)$$

where  $l$  is the original gauge length. In order to simplify the analysis, the circular cross section of the coupon was modelled as rectangular with the same area. Table 1 summarizes the input parameters of the numerical analysis.

### **3. NUMERICAL STUDY COMPARISONS**

The proposed methodology to obtain the creep-free material laws was applied with the explicit creep models to simulate the selected experimental tests. This section presents the numerical results of these simulations. The comparison between the numerical and experimental results illustrates the benefits of having explicit creep strain consideration. Three characteristic stress levels: low-stress (50-100 MPa), mid-stress (150-200 MPa) and high-stress (250-270 MPa) are chosen as the basis of the comparison.

#### **3.1 Comparison of simulation with Kirby & Preston [18]**

Figure 5 presents the results of the transient test simulations that were conducted using the stress-creep strain curves shown in Figures 3b and 3c with the Ramberg-Osgood skeleton curves for S275 steel taken from the study conducted by Kirby and Preston [18].

Figure 6 shows the results of transient coupon simulations conducted with the stress-creep strain curves shown in Figure 3f, together with the Eurocode 3 skeleton law for steel S275 from the Kirby & Preston study [18].

Figure 7 presents the results of transient coupon test simulations carried out with stress-creep strain curves determined with creep models Cr\_1 and Cr\_2 and the Ramberg-Osgood skeleton law for steel S355 from study [18].

Figure 8 presents the results of transient coupon test simulations conducted with stress-creep strain curves determined with the creep model Cr\_1 and the Eurocode 3 (bilinear-elliptic) skeleton law for steel S355 from study [18].

Table 2 compares the results from simulations from Figures 7b and 8c for different modelling schemes.

### **3.2 Comparison of results with Boko et al. [20]**

Figure 9 presents the results of transient coupon simulations that were conducted with stress-creep strain curves determined with creep model Cr\_2, using the chosen skeleton laws for steel S355 from Boko et al. [20].

Further verification of the proposed methodology is presented in Figures 10 and 11, which compares the numerical results with the series of transient tests conducted at heating rates of 5°C/min and 20°C/min from Kirby & Preston [18] for steel grades S275 and S355.

Table 3 presents the comparison of results between simulations from Figures 10c-10d for the different modelling schemes.

## **4. DISCUSSION OF THE RESULTS**

### **4.1 Validity of the proposed methodology**

It can be seen from Figures 5-9 that the analysis using the creep-free methodology provides strain-temperature curves with less total coupon strain compared to the corresponding experimental ones. The provision of an explicit creep model embodying the creep-free methodology into structural fire analysis results in stress-strain-temperature curves similar to those obtained from the corresponding implicit (skeleton) stress-strain laws. This similarity between implicit and creep-free analysis results occurs only if the appropriate type of stress-creep strain curve (determined by the creep model which is used for explicit creep modelling) is utilized in the creep-free analysis. The inclusion of the fourth term in the Equation (17) clearly gives the same results as subtraction of the skeleton stress-strain curve (the fourth step from Figure 1). It can be observed that some of the creep-free curves are lightly distorted in the temperature region 500-600°C (Figures 7b and 7c) if Cr\_1 is used as a background model for steel S355. This local distortion is caused by the stress-creep strain curves having been determined using creep models which calculate creep strains above 400°C. These local distortions are not physically-based, and illustrate

that a discrepancy exists when using the selected creep models in removing implicit creep from the Eurocode 3 stress-strain law in this limited temperature range.

## **4.2 Stress level**

At low stress levels, implicit stress-strain laws seem adequate for describing the evolution of creep for steel grades of S275 and S355, as can be seen in Figures 5-9. A combination of an implicit stress-strain law and an explicit creep model can also provide reasonable predictions at low stress levels. This can be attributed to the relatively low amount of creep strain at these stress levels, because of the short time-scale of the coupon tests. Creep strain at low stress level may become significant if the heating rate is lowered below 5°C/min, so that the period within which the transient test is conducted is increased.

At mid-range stress levels, the implicit stress-strain law seems to over-predict the creep strain level and further combination with an explicit creep model makes the predictions even worse. A creep-free material law derived by the proposed methodology, combined with a proper creep model, is capable of providing closer predictions to experimental results than the implicit (skeleton) stress-strain law for S275 and S355 steels.

At high levels of stress, the over-prediction of the creep strain using implicit (skeleton) stress-strain curves in analysis is even more pronounced. However, the application of the creep-free methodology at very high stress levels cannot accommodate the inherent implicit creep, since the creep derived from transient tests at a high stress is small because “runaway” strain rates arrive quickly. The fast arrival of runaway strain at high stress level may also be attributed to the existence of Lüders strain as well.

Another reason for over-prediction of total strain may be that the classical implicit stress-strain laws were framed so that the runaway failure occurs prematurely at high stress levels. This is particularly observed for simulations conducted using the Eurocode 3 stress-strain curves.

### **4.3 Type of stress-strain law**

It can be seen from Figures 5-9 that both the Eurocode 3 and Ramberg-Osgood stress-strain models provide satisfactory predictions of the total strain. However, it can be observed that at high stress levels the Eurocode 3 stress-strain law under-predicts the total strain for steel grades S275 and S355. This can be interpreted as due to the inherently conservative nature of the Eurocode 3 stress-strain curves as part of a design code. If the Eurocode 3 stress-strain curves are used in conjunction with force-control solvers, the total strain prediction over the strain level of 2% is not possible. However, the Ramberg-Osgood stress-strain law can provide the creep strain prediction in the 2-5% strain interval and beyond, because it has a monotonic increase in the higher-strain region.

### **4.4 Heating rate**

Figures 10 and 11 show that the creep-free methodology provides good results compared to the results of transient tests conducted at heating rates between of 5°C/min and 20°C/min. This illustrates that the proposed methodology is applicable to heating rates other than 10°C/min. As can be seen in Figures 10 and 11, with a range of heating rates, the proposed “creep-free” methodology shows better correlation with the experimental results than using the skeleton stress-strain law in combination with an explicit creep model.

### **4.5 Acceptability of the selected creep models**

This study has shown that creep model Cr\_3 can correlate well with the experimental results for steel grade S275 from reference [18], Cr\_2 is applicable to steel grade S355 from the same study, and that Cr\_2 is able to recreate reasonably well the experimental results from reference [20] for steel grade S355. The amount of creep strain indicated by the chosen creep models can be regarded as a good representation for the level of creep strain that was present in the selected coupon test studies.

## 4.6 Application of the creep-free methodology in structural fire analysis

The application of the creep-free methodology and its benefits in structural fire analysis can be illustrated by using the proposed methodology in numerical modelling of the fire test of specimen E2 from the study by Torić et al. [7]. The simply supported steel beam of Grade S355 was partially heated over its length at an average heating rate of approximately 3.5°C/min. Heating curves for the upper and lower flanges of the beam at mid-span are presented in Figure 12. The beam was loaded with a vertical force of 400 kN at mid-span and a horizontal compressive force of 200 kN. Reduction factors for yield strength and modulus of elasticity of the steel used in the beam have been determined experimentally [20], and subsequently used in the numerical model. Hence, genuine material properties are accounted for in the analysis.

In order to illustrate the benefit of using the creep-free methodology, member E2 was analysed using all three explicit creep models, together with the implicit Eurocode 3 stress-strain law and with a creep-free Eurocode 3 model. The results using both implicit and creep-free methodologies are presented in Figure 13. Comparison of the results from the creep-free analysis with the implicit-creep analysis and explicit consideration of creep indicates that there are significant discrepancies in the deflection response and the fire resistance prediction of the selected steel beam using these analysis strategies. Creep-free analysis, in combination with explicit creep model Cr\_2, has shown very good correlation with the test results, emphasizing the applicability of this model to steel S355. An additional factor, which might potentially influence the modelling results, is the variation of yield strength due to localised variations in chemistry and production processes of steel.

## 5. CONCLUSIONS

A proposed methodology to create creep-free stress-strain material laws (referred to as a “creep-free” methodology) has been presented in this paper. On the basis of a series of

numerical models of various experimental tests, it has been demonstrated that the proposed “creep-free” methodology can provide a better correlation with the experimental results for contemporary structural steel grades than the commonly-used implicit stress-strain laws, which generally over predict creep strain evolution. Creep can be explicitly modelled in fire engineering analysis by combining the creep-free stress-strain material laws obtained by the proposed methodology with a proper explicit creep model. This combination excludes the implicit consideration of the creep strain in the commonly-used stress-strain laws.

The proposed methodology can be used to extract implicit creep from any type of steel stress-strain law determined by a transient test at certain heating rate, provided that a material creep model is determined in advance. A selection of creep models used in this study has proved sufficiently accurate for extracting implicit creep from the fire analyses conducted, although there is some discrepancy in the temperature region 500-600°C for certain creep-free simulations. Further research is planned to explore the level of conservativeness which is inherent in the Eurocode 3 implicit stress-strain law, and to find a suitable modified Eurocode 3 creep-free law which correlates with the results from this study.

## **Acknowledgement**

The principal author would like to thank the University of Split, Faculty of Civil Engineering, Architecture and Geodesy for their financial support during the research period.

## **6. REFERENCES**

- [1] Poh, K. W., “Stress-Strain-Temperature Relationship for Structural Steel”, *Journal of Materials in Civil Engineering*, 2001; 13(5):371-379.
- [2] ASCE, “Structural fire protection” ASCE committee on fire protection, Manual No. 78, ASCE, Reston, Va., 1992.
- [3] EN 1993-1-2:2005, “Eurocode 3 - Design of steel structures - Part 1-2: General Rules - Structural fire design”, European Committee for Standardization, Brussels, 2005.



- [4] EN1992-1-2:2004, "Eurocode 2 - Design of Concrete Structures - Part 1-2: General Rules - Structural Fire Design", European Committee for Standardization, Brussels, 2004.
- [5] Kodur, V. K. R. and Dwaikat, M. M. S., "Response of steel beam–columns exposed to fire", *Engineering Structures*, 2009; 31(2):369-379.
- [6] Kodur, V. K. R., Dwaikat, M. M. S. and Fike, R., "High-Temperature Properties of Steel for Fire Resistance Modeling of Structures", *ASCE Journal of Materials in Civil Engineering*, 2010; 22(5):423-434.
- [7] Torić, N., Harapin, A. and Boko, I., "Experimental Verification of a Newly Developed Implicit Creep Model for Steel Structures Exposed to Fire", *Engineering Structures*, 2013; 57:116-124.
- [8] Li, G.-Q. and Zhang, C., "Creep Effect on Buckling of Axially Restrained Steel Columns in Real Fires", *Journal of Constructional Steel Research*, 2012; 71:182-188.
- [9] Morovat, M. A., Lee, J., Engelhardt, M. D., Taleff, E. M., Helwig, T. A., Segrest, V. A., "Creep Properties of ASTM A992 Steel at Elevated Temperatures", *Advanced Materials Research*, 2012; 446-449:786-792.
- [10] Morovat, M. A., Engelhardt, M. D., Helwig, T. A., Taleff, E. M., "High-Temperature Creep Buckling Phenomenon of Steel Columns Subjected to Fire", *Journal of Structural Fire Engineering*, 2014; 5(3):189-202.
- [11] Harmathy, T. Z., "Creep Deflections of Metal Beams in Transient Heating Processes, with Particular Reference to Fire", *Canadian Journal of Civil Engineering*, 1976; 3(2):219-228.
- [12] Harmathy, T. Z., "A Comprehensive Creep Model", *Journal of Basic Engineering*, 1967, 89(3): 496-502.
- [13] Plem, E., "Theoretical and experimental investigations of point set structures", Swedish Council for Building Research, Document, D9, 1975.
- [14] Harmathy, T. Z. and Stanzak, W.W., "Elevated-Temperature Tensile and Creep Properties of Some Structural and Prestressing Steel", National Research Council of Canada, Division of Building Research, Ottawa, 1970.
- [15] Shepherd, P., "The performance in fire of restrained columns in steel-framed construction", Ph.D. Thesis, University of Sheffield, 1999.
- [16] Burgess, I.W., El-Rimawi, J.A. and Plank, R.J., "A secant stiffness approach to the fire analysis of steel beams", *Journal of Constructional Steel Research*, 1988; 11:105-120.
- [17] Mäkeläinen, P., Outinen, J. and Kesti, J., "Fire design model for structural steel S420M based upon transient-state tensile test results", *Journal of Constructional Steel Research*, 1998, 48; 47–57.

- [18] Kirby, B.R. and Preston, R.R., “High Temperature Properties of Hot-Rolled, Structural Steels for Use in Fire Engineering Design Studies”, *Fire Safety Journal*, 1988, 13:27-37.
- [19] Anderberg, Y., “Modelling Steel Behaviour”, *Fire Safety Journal*, 1988; 13(1):17-26.
- [20] Boko, I., Torić, N. and Peroš, B., “Structural fire design parameters and procedures – analysis of the potential of Eurocode 3”, *Materialwissenschaft und Werkstofftechnik*, 2012; 43(12):1036-1052.
- [21] Huang, Z., Burgess, I.W. and Plank, R.J., “Three-dimensional analysis of reinforced concrete beam-column structures in fire”, *ASCE Journal of Structural Engineering*, 2009; 135(10):1201-1212.
- [22] Cai, J., Burgess, I.W. and Plank, R.J., “A generalised steel/reinforced concrete beam-column element model for fire conditions”, *Engineering Structures*, 2003; 25(6):817-833.

## Figure Captions

- Figure 1: Flow-chart for creation of a creep-free stress-strain law
- Figure 2: Simulated temperature-creep strain curves for S275 using; (a-c) Ramberg-Osgood and (d-f) Eurocode 3 skeleton laws with different creep models at 10°C/min.
- Figure 3: Simulated stress-creep strain curves for S275 using; (a-c) Ramberg-Osgood and (d-f) Eurocode 3 skeleton laws with different creep models at 10°C/min.
- Figure 4: Key dimensions of coupon [20] and the beam element segmentation.
- Figure 5: Comparison of results of modelling coupon tests at 10 °C/min between creep-free and implicit creep analyses using Ramberg-Osgood law for steel S275 from Kirby & Preston [18].
- Figure 6: Comparison of results of modelling coupon tests at 10 °C/min between creep-free and implicit creep analyses using Eurocode 3 law for steel S275 from Kirby & Preston [18].
- Figure 7: Comparison of results of modelling coupon tests at 10 °C/min between creep-free and implicit creep analyses using Ramberg-Osgood law for steel S355 from Kirby & Preston [18].
- Figure 8: Comparison of results of modelling coupon tests at 10 °C/min between creep-free and implicit creep analyses using Eurocode 3 law for steel S355 from Kirby & Preston [18].
- Figure 9: Comparison of results of modelling coupon tests at 10 °C/min between creep-free and implicit creep analyses using; (a-c) Ramberg-Osgood and (d-f) Eurocode 3 laws and creep model Cr\_2 for steel S355 from Boko et al. [20].
- Figure 10: Comparison of results of modelling coupon tests at 5 °C/min between creep-free and implicit creep analyses using Ramberg-Osgood and Eurocode 3 laws from Kirby & Preston [18].
- Figure 11: Comparison of results of modelling coupon tests at 20 °C/min between creep-free and implicit creep analyses using Ramberg-Osgood and Eurocode 3 laws from Kirby & Preston [18].
- Figure 12: Heating curves for upper and lower flange at mid-span of the analysed beam.
- Figure 13: Application of the creep-free analysis and comparison with test results using selected creep models

## **Table Captions**

Table 1: Input parameters for the numerical analysis.

Table 2: Accuracy of creep-free methodology in predicting total strain from Figures 7b and 8c for steel S355 at 150 MPa using selected stress-strain laws.

Table 3: Accuracy of creep-free methodology in predicting total strain from Figures 10c-10d for steel S355 at 150 MPa.

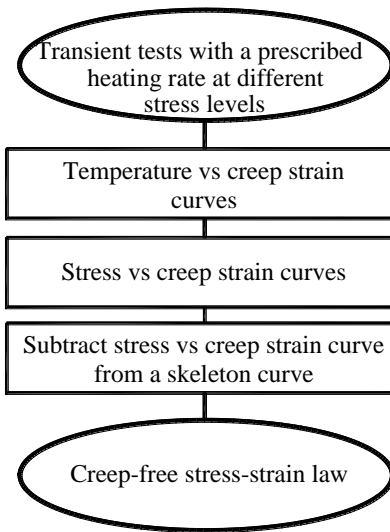


Figure 1

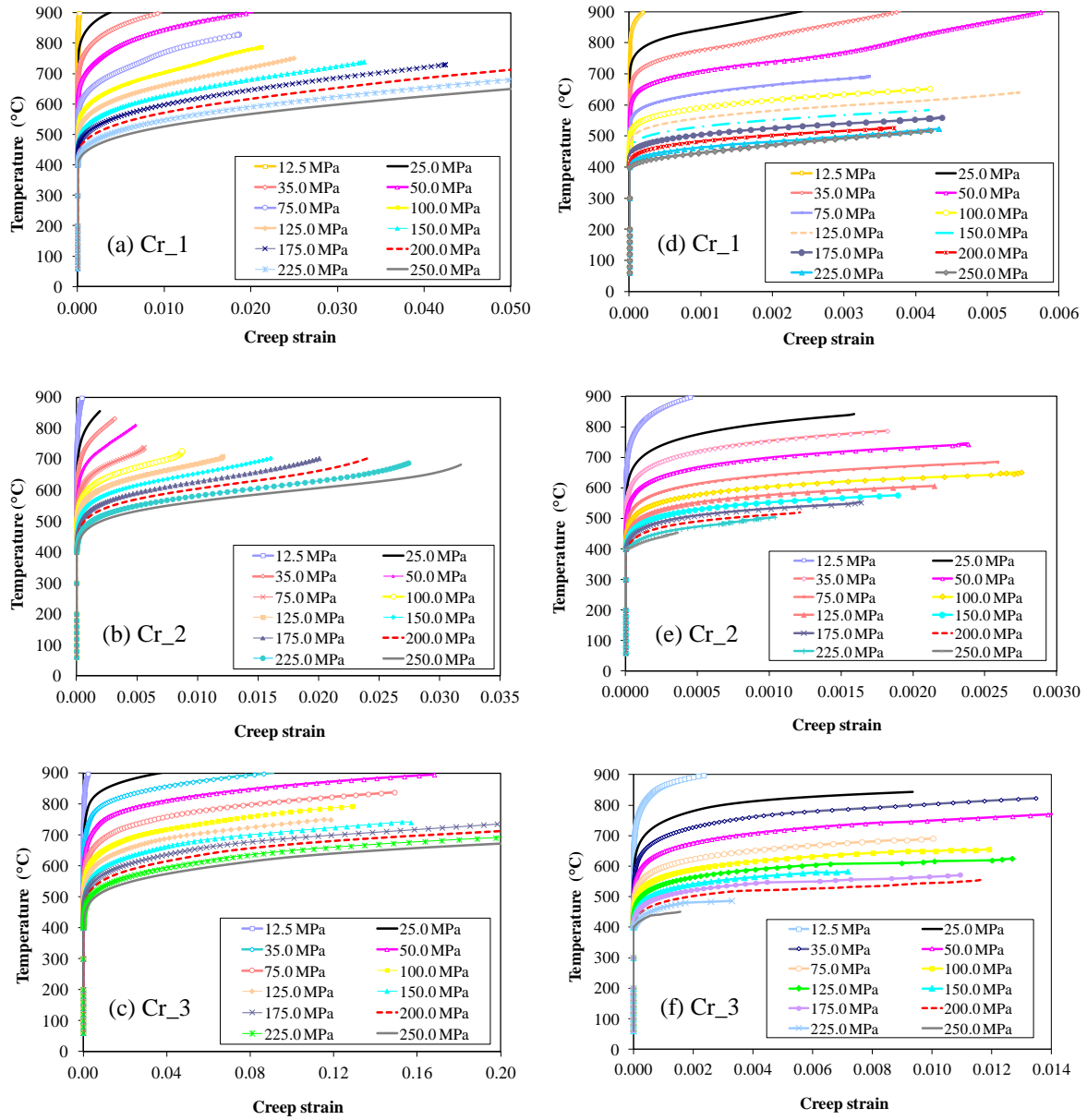


Figure 2

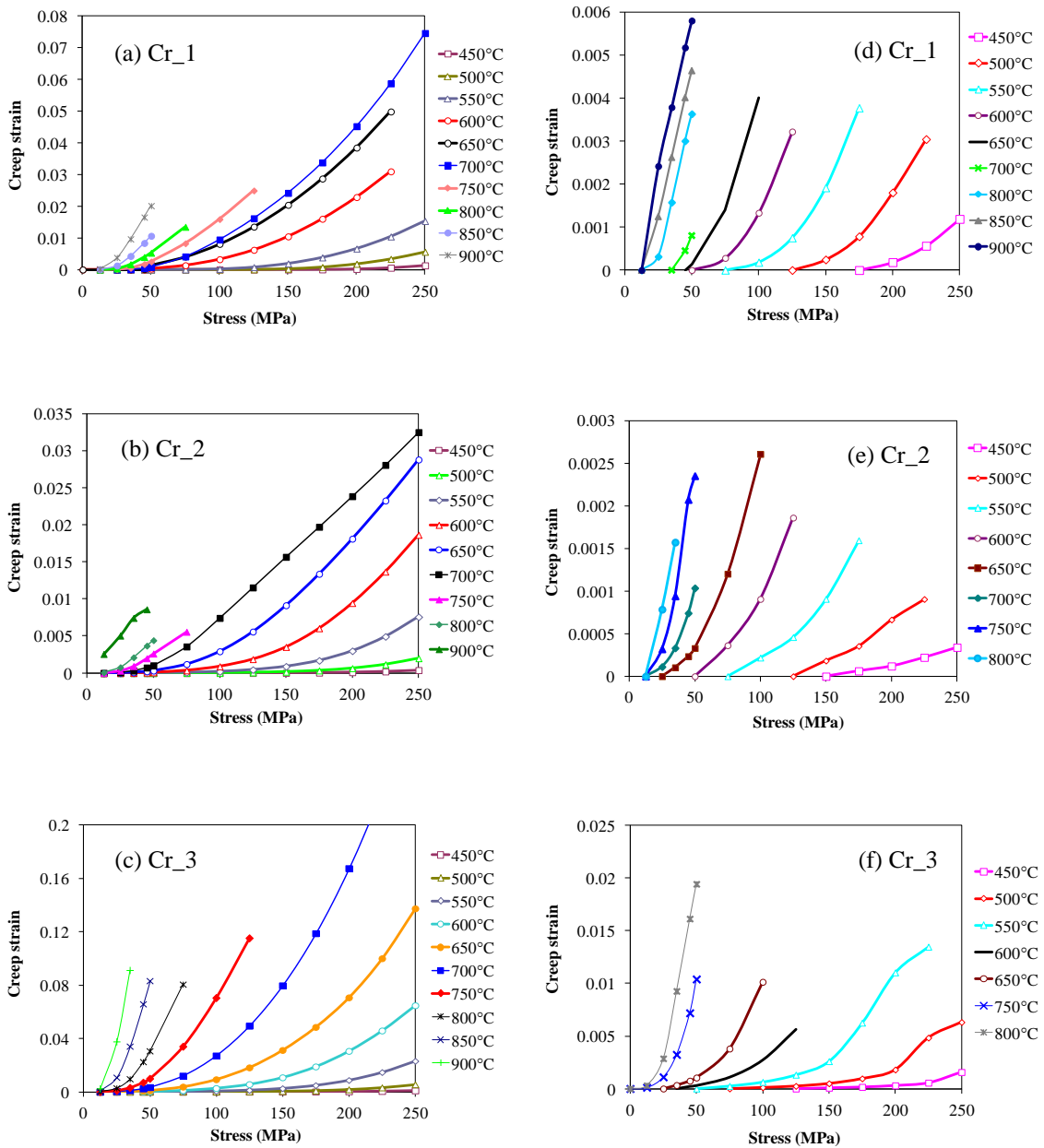
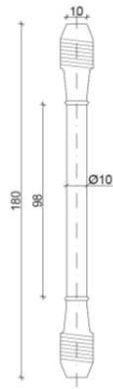
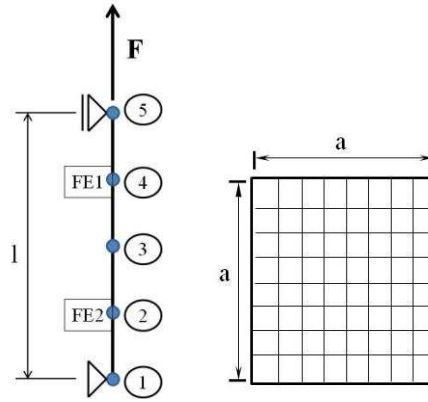


Figure 3



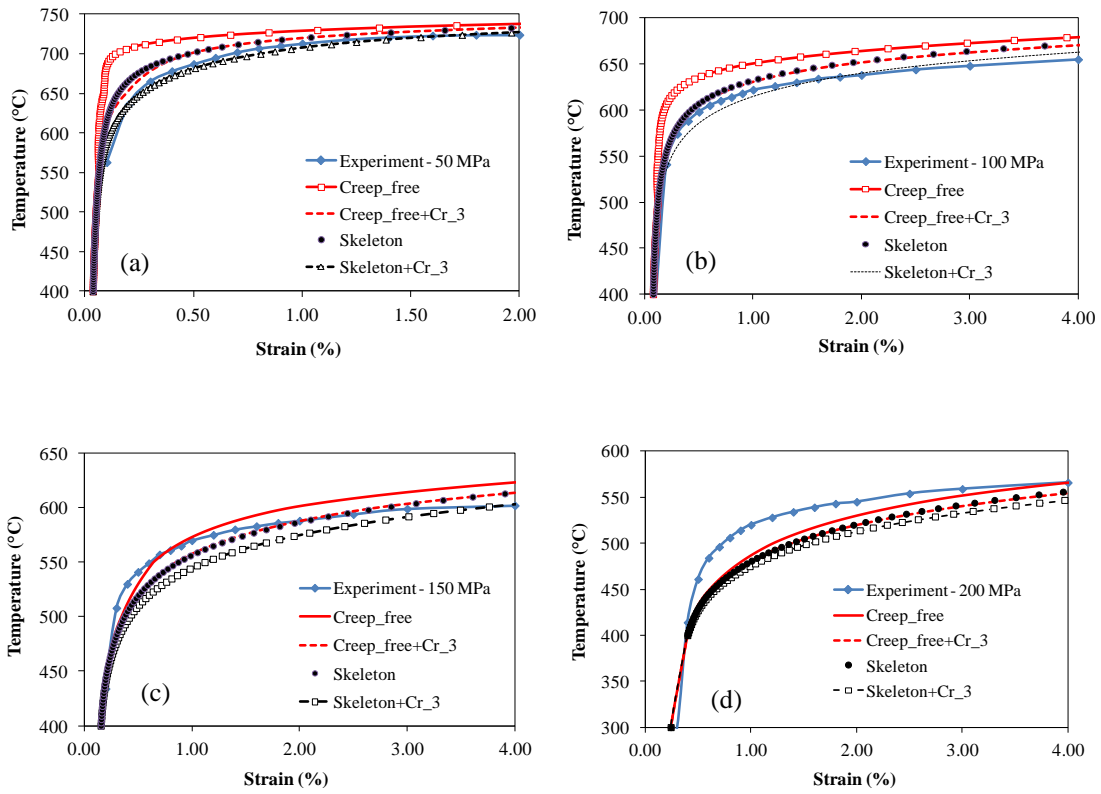
(a) Coupon shape [20]



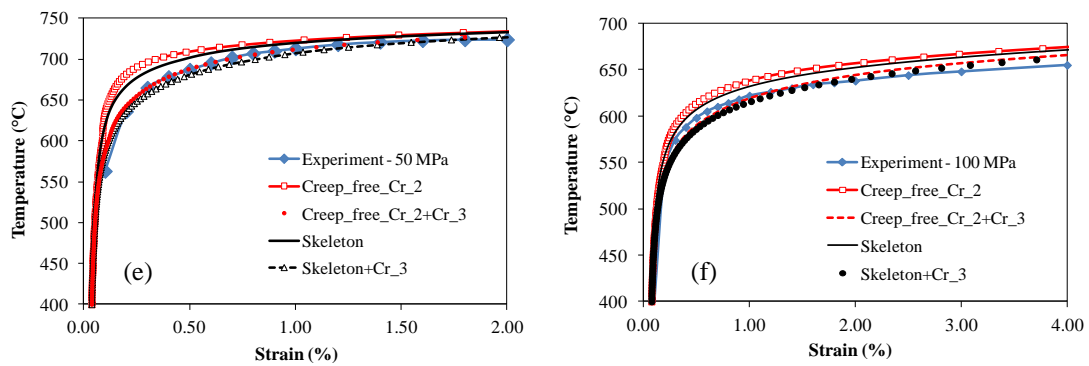
(b) Vulcan finite element mesh

Figure 4



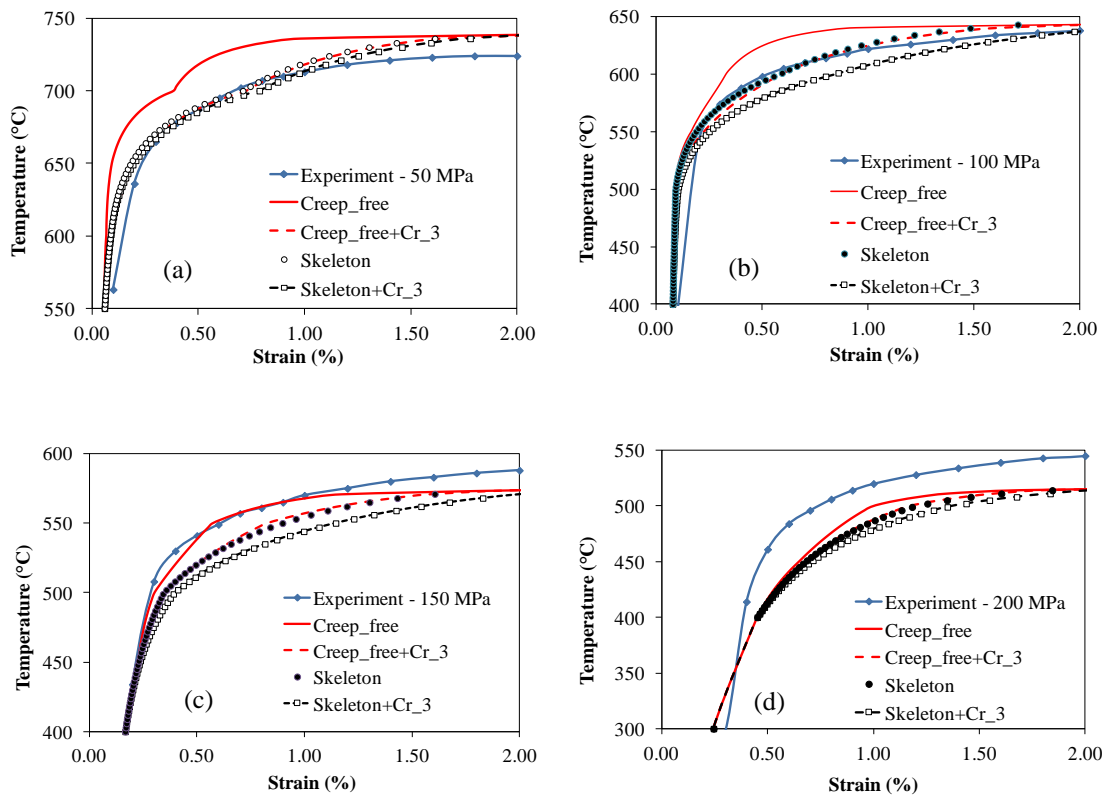


(a-d) 10°C/min and creep-free analyses using creep data from Fig 3c; 50-200 MPa.



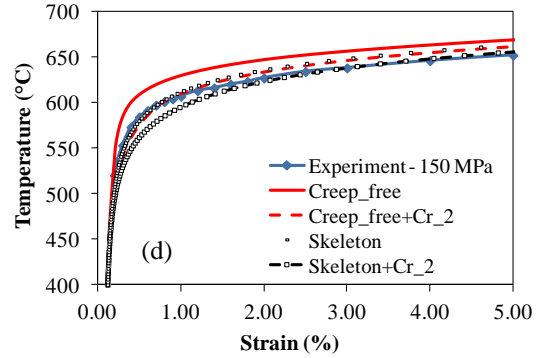
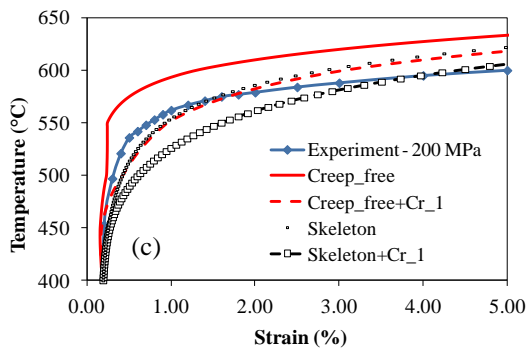
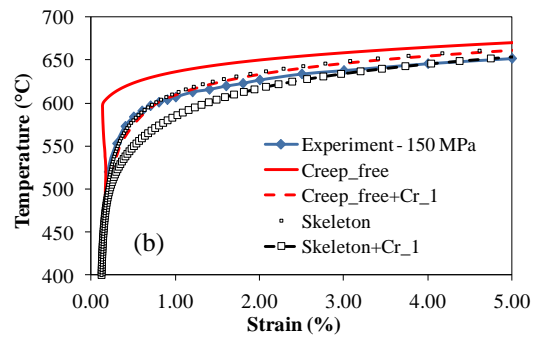
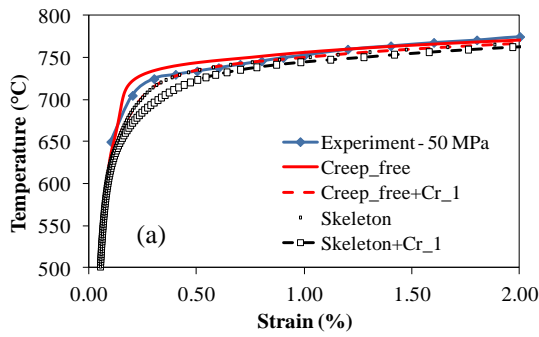
(e-f) 10°C/min and creep-free analyses using creep data from Fig 3b; 50-100 MPa.

Figure 5

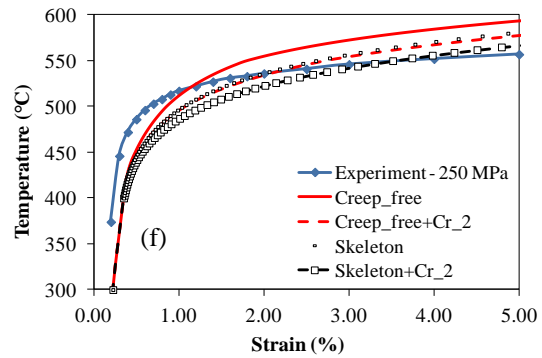
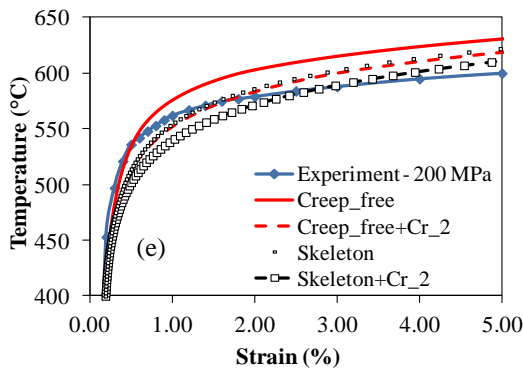


(a-d) Creep data from Fig 3f at 50-200 MPa.

Figure 6

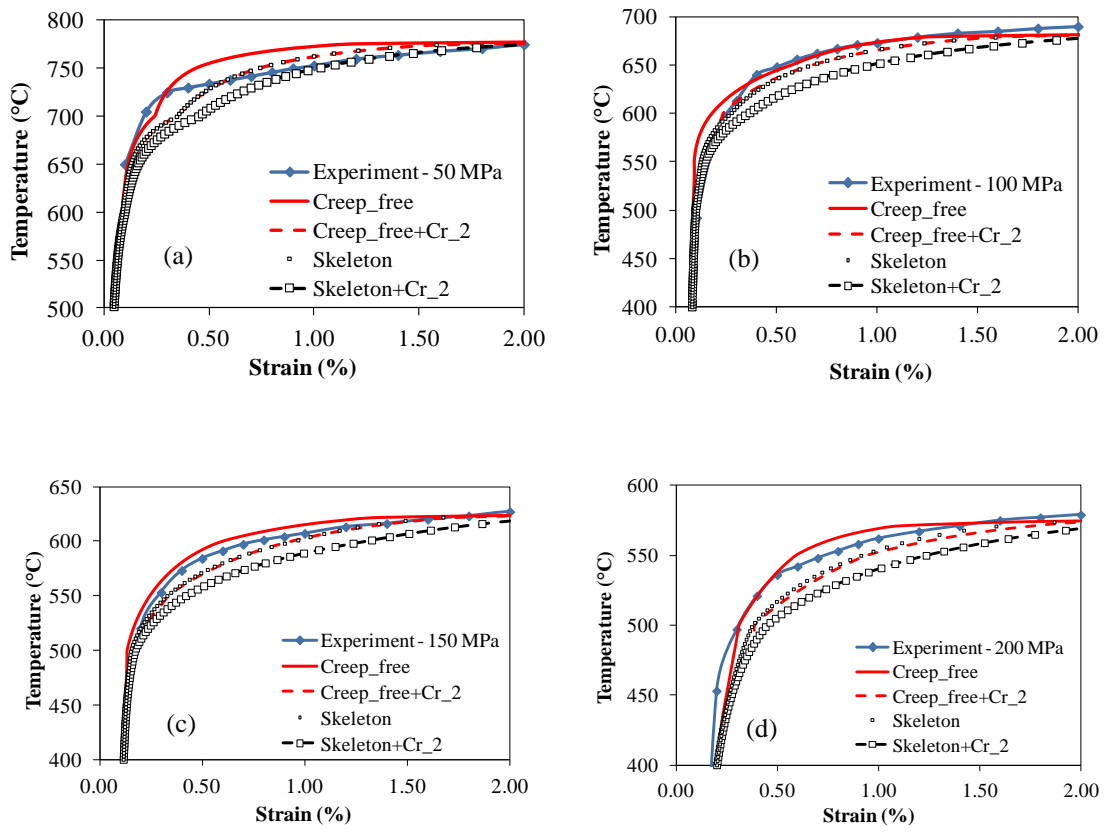


(a-c) Creep model Cr\_1 at 50-200 MPa.



(d-f) Creep model Cr\_2 at 150-250 MPa.

Figure 7



(a-d) Creep model Cr\_2 at 50-200 MPa.

Figure 8

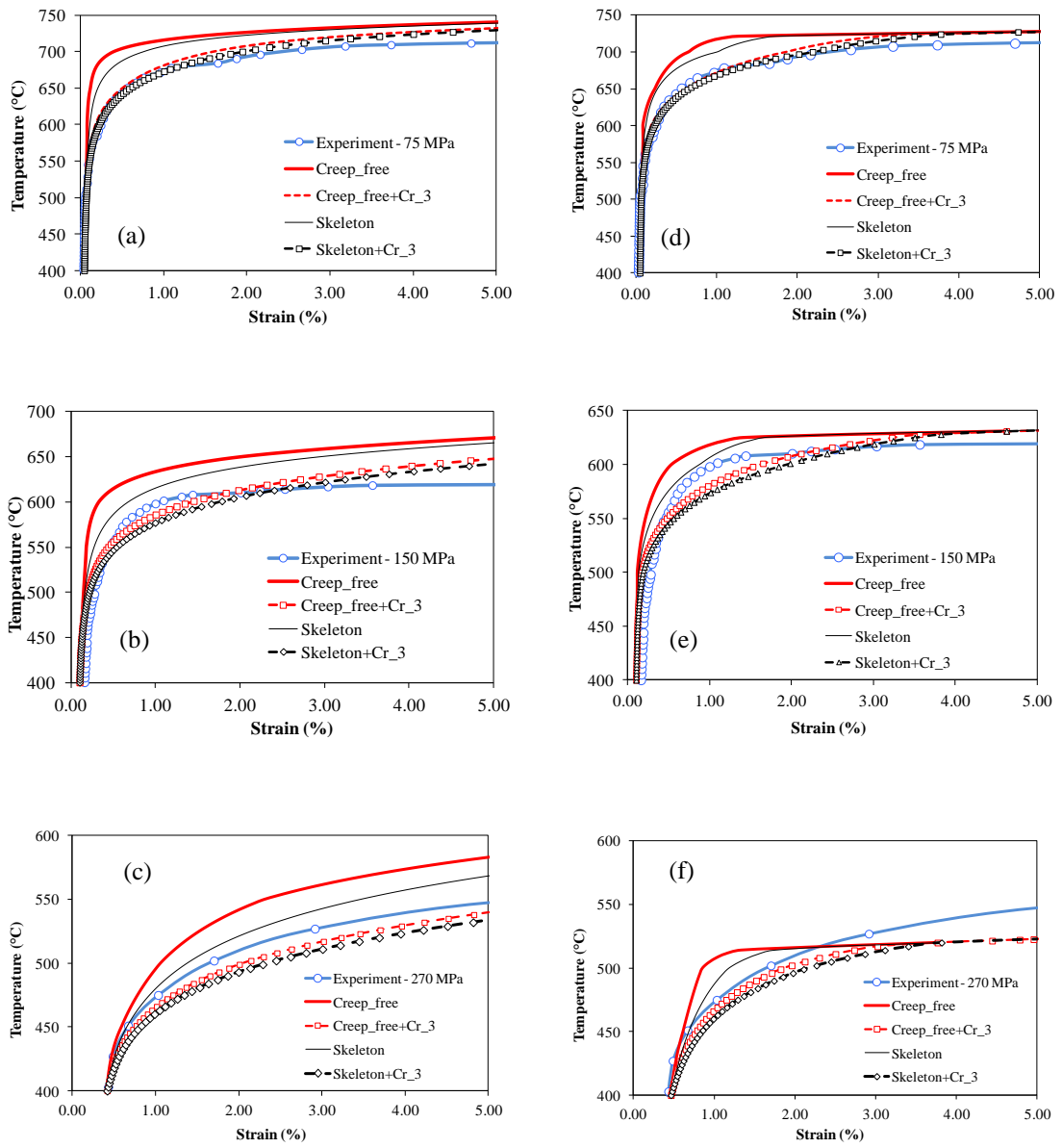
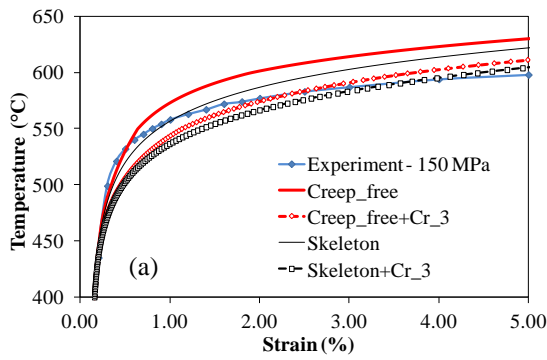
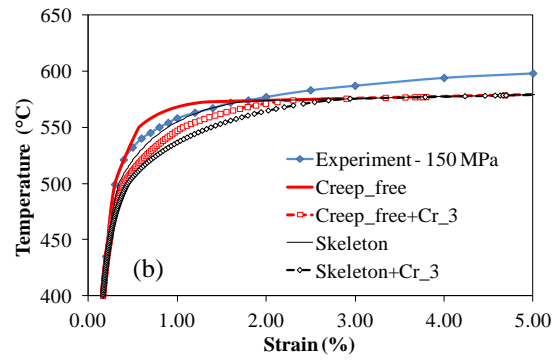


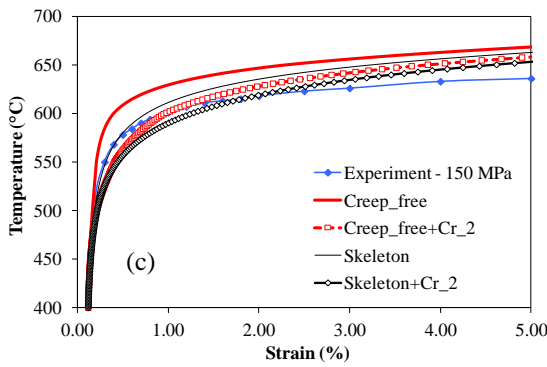
Figure 9



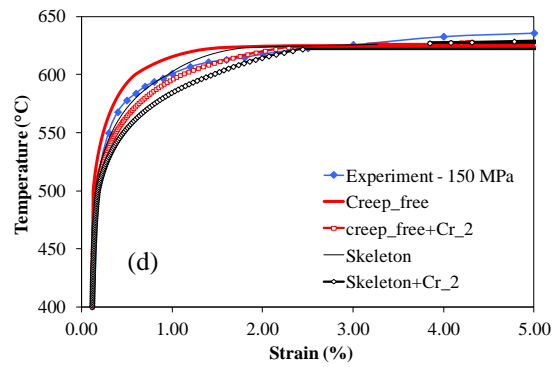
(a) S275; Ramberg-Osgood skeleton law and creep-free analysis using creep data from Fig 3c at 150 MPa.



(b) S275; Eurocode 3 skeleton law and creep-free analysis using creep data from Fig 3f at 150 MPa.

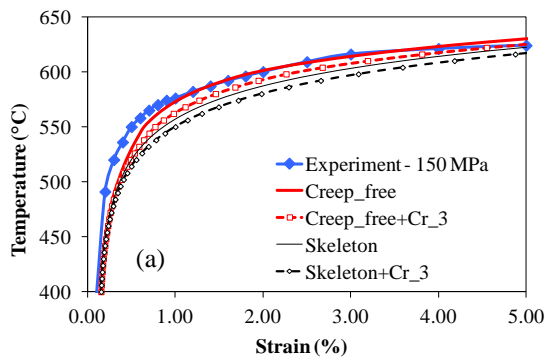


(c) S355; Ramberg-Osgood skeleton law and creep-free analysis using creep model Cr\_2 at 150 MPa.

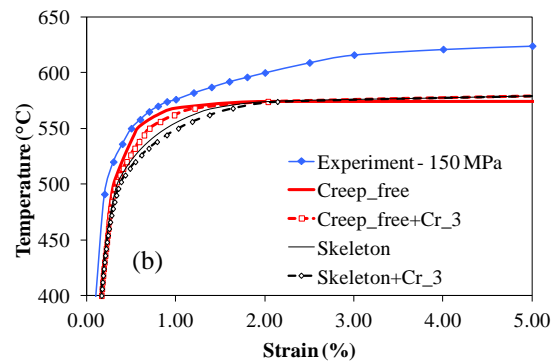


(d) S355; Eurocode 3 skeleton law and creep-free analysis using creep model Cr\_2 at 150 MPa.

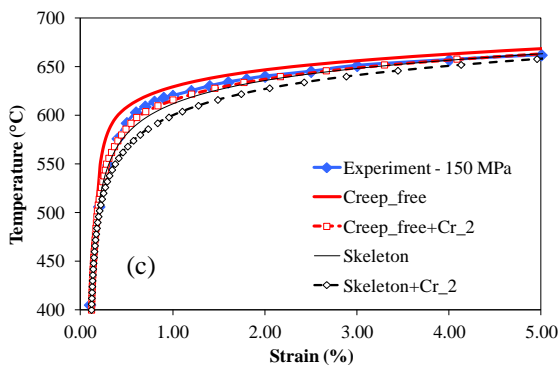
Figure 10



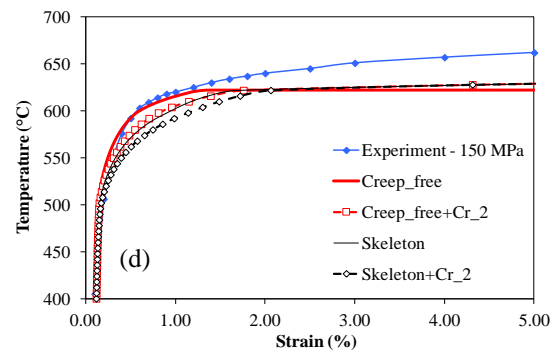
(a) S275; Ramberg-Osgood skeleton law and creep-free analysis using creep data from Fig 3c at 150 MPa.



(b) S275; Eurocode 3 skeleton law and creep-free analysis using creep data from Fig 3f at 150 MPa.



(c) S355; Ramberg-Osgood skeleton law and creep-free analysis using creep model Cr\_2 at 150 MPa.



(d) S355; Eurocode 3 skeleton law and creep-free analysis using creep model Cr\_2 at 150 MPa.

Figure 11

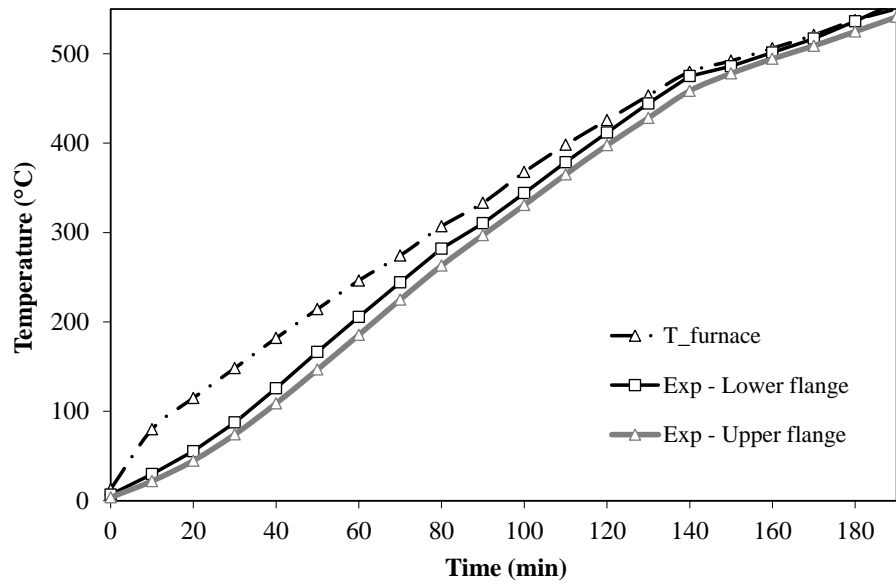


Figure 12



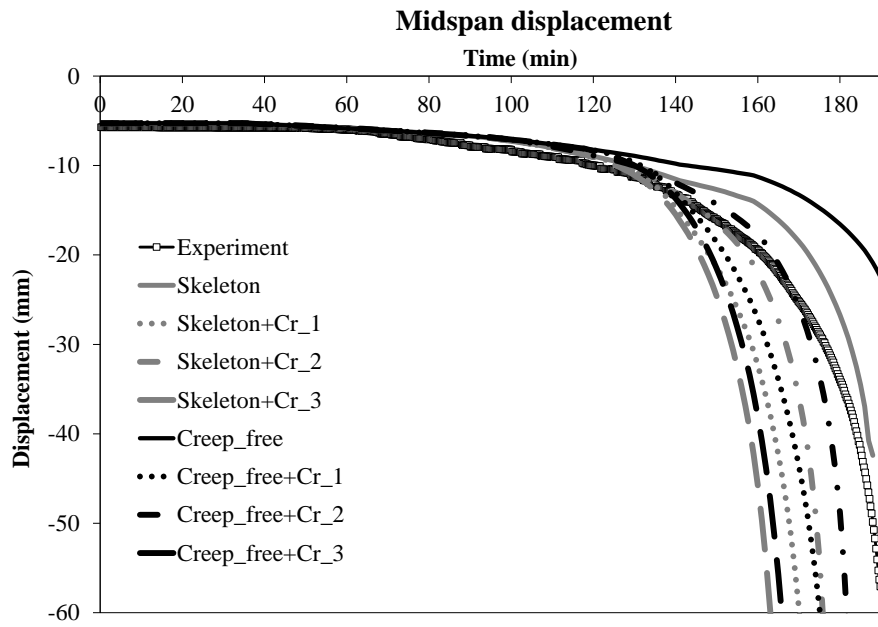


Figure 13

Table 1

Study		Yield strength - 20°C (MPa)	Modulus of elasticity - 20°C (MPa)	Incremental time step $\Delta t$ (min)	Gauge length l (mm)	Rectangular section length a (mm)
Kirby & Preston [18]	S275	267.0	185000.0	0.3	40	7.07
	S355	357.0	185000.0			
Boko et al. [20]	S355	362.4	209000.0	0.3	98	8.86

Table 2

Temperature (°C) / Strain (%)	Exp [18]	Ramberg_Skeleton + Cr_1	EC3_skeleton + Cr_2	Ramberg_creep_free + Cr_1	EC3_creep_free + Cr_2
607	1.00	1.58	1.51	0.93	1.17
613	1.20	1.80	1.73	1.09	1.40
616	1.40	1.93	1.86	1.19	1.54
620	1.60	2.12	2.09	1.32	1.78
623	1.80	2.28	2.33	1.47	2.10
627	2.00	2.51	3.71	1.61	3.84

Table 3

Temperature (°C) / Strain (%)	Exp [18]	Ramberg_Skeleton + Cr_2	EC3_skeleton + Cr_2	Ramberg_creep_free + Cr_2	EC3_creep_free + Cr_2
601	1.00	1.28	1.47	0.94	1.13
607	1.20	1.48	1.68	1.09	1.34
611	1.40	1.63	1.83	1.21	1.51
613	1.60	1.71	1.92	1.27	1.60
615	1.80	1.80	2.01	1.34	1.70
618	2.00	1.94	2.18	1.46	1.86